MODELLING OF CHROMATIC ABERRATION FOR HIGH PRECISION PHOTOGRAMMETRY

Thomas Luhmann, Heidi Hastedt, Werner Tecklenburg

Institute for Applied Photogrammetry and Geoinformatics
University of Applied Sciences Oldenburg, Germany - luhmann@fh-oow.de

Commission V, WG V/1

KEY WORDS: RGB, colour, calibration, chromatic aberration, precision, accuracy

ABSTRACT:

Chromatic aberration appears for almost all lenses for imaging based on white light. The effect degrades image quality for both b/w and colour cameras. This paper discusses the possibilities of modelling chromatic aberration with self-calibrating bundle adjustment for high-precision photogrammetric 3D point measurement using all three channels of a true colour image. After a survey on common types of digital colour sensors, wave-length dependent imaging errors of usual lenses are discussed. Consequently, different options for the correction of the occurring effects are derived. The resulting effect on image and object accuracy is verified by various test field calibrations using different combinations of digital colour cameras and lenses. For standard imaging configurations in close-range photogrammetry, a significant enhancement of inner precision by a factor of 1.7 can be proven. It can be shown that the length measurement error for standardized imaging configurations can be improved slightly whereby final results are still on investigation.

1. INTRODUCTION

With the introduction of high-resolution still-video cameras during the 1990ies only black and white cameras were available. Their potential for accurate photogrammetric measurements was shown quite early (e.g. Peipe 1995, Shortis & Beyer 1996). Although these cameras were restricted by a number of technical limitations, the total physical sensor resolution could be used for image data and processing. With the increasing use of digital consumer cameras the image resolution was enhanced to recently up to 20 Mega pixels for SLR cameras and camera backs. Sensors with more than 40 Mega pixels have been announced already. On the other hand, pure b/w cameras are practically not available for off-the-shelf cameras, except for specialised and expensive metric cameras (e.g. GSI Inca). In contrast, digital video cameras with up to 1300 x 1000 pixels are widely available also in b/w.

In industrial photogrammetric 3D metrology high-resolution SLR cameras are usually used for off-line applications. Most photogrammetric image analysis programs are not able to process true colour pictures but, they are restricted to work with only one colour channel (usually green) or with converted grey level (intensity) images. Hence, a loss of geometric resolution occurs as a function of the colour sensor and the post-processing of the image data, either within the camera firm ware or off-line. Thus, a reduced image and object point accuracy can be expected.

In addition, wave-length depending imaging errors of the optical components and different characteristics in colour channels yield to various geometric errors of the colour image. First of all, the chromatic aberration is to be mentioned. On the one hand, it occurs as a longitudinal error yielding different focal lengths and focusing image distances. On the other hand, the transversal chromatic aberration results in different scales perpendicular to the optical axis as a function of the image radius (distance of a point from the optical axis). The latter effect is identical to radial-symmetric distortion which is not only a function of wave length and refraction but also of size and position of the aperture.

This paper deals with possibilities for the optimisation of the photogrammetric object point measurement by using colour information of the three RGB channels and consideration of chromatic aberration. First results of the study have been published in Hastedt et al., 2006. The long-term objective is to achieve the same accuracy level as with an equivalent b/w sensor.

2. COLOUR CAMERAS AND IMAGING SENSORS

As usually known a true colour image consists of three channels in red, green and blue (RGB). Most cameras deliver either images in raw formats, i.e. uncompressed image data with full geometric and radiometric resolution, or in standardised formats (e.g. TIFF, JPEG) that may be subject to information loss.

Digital colour sensors are usually working after one of the following principles (overview in Luhmann et al., 2006):

a) RGB separation by colour filter masks that are mounted onto the light-sensitive sensor area;
b) RGB separation by using a full colour sensor that consists of three sensitive layers similar to an analogue film.

Option a) is based on filter masks where adjacent pixels are sensible for a specific wave-length range. The most popular filter mask is the Bayer pattern that uses, in a 2x2 neighbourhood, one pixel for red, one for blue, and two for green (see Fig. 1). The higher weight for green is adapted to the maximum sensitivity of yellow and green of the human eye. Recently cameras are offered by Sony that are equipped with a four colour filter mask in red, green, blue and emerald. Fuji has developed a diagonal arrangement of sensor pixels that are completed by smaller pixels for light intensity only.

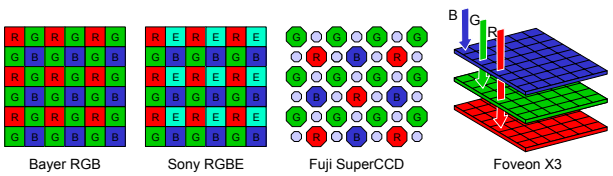

Fig. 1: Layout of different colour sensors

A completely different technology is offered by the Foveon sensors that use three colour layers. Per se, each pixel registers a true RGB value, thus the geometric resolution is about two times higher than for Bayer type sensors (Lyon & Hubel, 2002). However, these sensors are available up to 2268 x 1512 pixels only.

3. OPTICAL IMAGING ERRORS

3.1 Distortion

Distortion is existing with practically each lens due to refraction (dispersion) in asymmetrically designed lenses, and the aperture. With respect to the position of the aperture, either pin-cushion or barrel type distortion appears. A centred aperture within a symmetrical lens yield a more or less distortion-free (orthoscopic) image (see Fig. 2). Since refraction is a function of wave length, also distortion depends on wave length (overview in Luhmann et al., 2006).

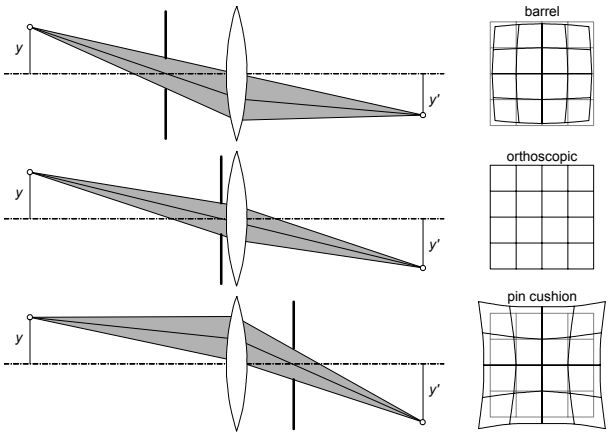

Fig. 2: Radial-symmetric distortion resulting from different aperture positions

In addition to radial-symmetric distortion the influence of decentric lenses is compensated by tangential and asymmetric correction functions. Imaging errors within the sensor plane or by electronic effects are not further discussed here.

Usually the photogrammetric correction polynomials for radial-symmetric distortion are determined by self-calibrating bundle adjustment. Since the principal distance is often calibrated as well, the parameters of radial-symmetric distortion (A_1, A_2, A_3 or K_1, K_2, K_3) are linear with respect to the principal distance, hence they can only be computed if either a second zero-crossing of the distortion polynomial is introduced (balanced distortion), or if the linear term of the function is eliminated.

For each bundle adjustment with self-calibration numerical correlations exist between the parameters of interior and exterior orientation. The correlations depend on the imaging configuration and the provided object information. They can yield to an effect that, for instance, the position of the projection centre in image space (c,x'_0,y'_0) can partly be modelled by a corresponding shift of the parameter of exterior orientation X0,Y0,Z0. Using plumbline calibration (Fryer & Brown, 1986), the distortion parameters can be determined without any correlation to exterior orientation.

3.2 Chromatic aberration

Chromatic aberration is caused by different paths of light through the lens system for each wave length. Longitudinal chromatic aberration yields different focal points for each wave length. A white object point is imaged with different image distances, hence no correct focus is possible (see Fig. 3). Depending on the lens quality this effect can be reduced by using different lens types and coatings. If the focusing plane is adjusted to a mean wave length (e.g. green), imaging errors in the red and blue range are minimised (see Pedrotti et al., 2002, Schröder, 1990).

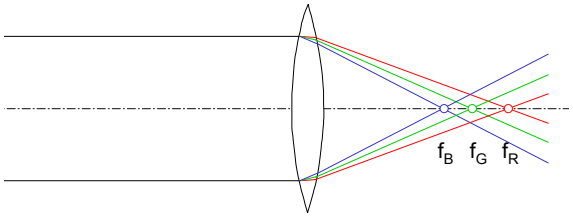

Fig. 3: Longitudinal chromatic aberration

In practice chromatic aberration yields to a degraded focusing quality. So-called achromats are lenses where chromatic aberration is reduced to a minimum due to a particular lens design. If white targets are used for photogrammetry, the longitudinal chromatic aberration does, in theory, not effect the position of the target centre in image space because white light consists of all wave lengths. If, however, coloured targets are used, e.g. red and green targets (see e.g. Cronk et al., 2006), these points are located in different image positions.

Transversal chromatic aberration causes an object to be imaged with different scales as a function of the image radius. For monochromatic light the effect is identical to radial distortion. For polychromatic light a radial shift of colours can be observed.

The effect can easily be shown for digital colour images. Fig. 4a displays the non-sufficient imaging quality of a white target in a colour image. Colour shift can easily be observed at the edges of the target pattern, as it would appear for every other object edge. Fig. 4b shows a sufficient quality of the green image as it may be used for photogrammetric point measurement. The difference image in Fig. 4c illustrates the colour shift between green and red channel.

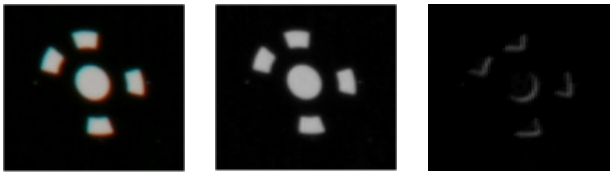

a) original RGB image b) green channel c) difference red-green

Fig. 4: Colour shifts for b/w edges

The shown colour shift yield to colour-dependent functions for radial-symmetric distortion. An example is displayed in Fig. 6. If the individual colour shift is known, the image can be resampled to a distortion or aberration free image. Commercial

programs with approximate solutions are available, e.g. Nikon Capture 4.4 or Adobe Photoshop CS2. A strict photogrammetric procedure is presented by Kaufmann & Ladstädter, 2005, and Schwalbe & Maas, 2006.

4. INVESTIGATIONS

The preliminary objective of the following empirical tests is to investigate the influence of chromatic aberration to image and object accuracy for typical test field calibrations. The experiments are performed with different high-resolution digital SLR cameras and different lenses. Finally, a procedure is suggested that uses colour information for a significant accuracy enhancement. These investigations do not aim to correct non-sufficient image quality of digital colour cameras by an optimized resampling of the RGB image.

4.1 Experimental setup

Table 1 summarizes the digital cameras and lenses that have been used for two different test field measurements. Test 1 uses an almost plane test field (1.0m x 1.0m x 0.5m) with about 100 targets and an optional scale bar that is imaged by an average of 18 images (Fig. 5a). For test 2 a 3D test field is measured by an average of 90 images according to VDI 2634 guideline (Luhmann & Wendt, 2000), see Fig. 5b.

Table 1: Cameras and lenses used for test field calibrations

Cameras	Pixel resolution	Sensor format [mm]	Focal length [mm]
Fuji S2 Pro	3040 x 2016	23.3 x 15.6	14, 20, 28
Canon EOS D1 MarkII	4992 x 3328	36,0 x 24.0	35
Nikon D2X	4288 x 2848	23.5 x 15.6	24
Sigma SD10	2268 x 1512	20.7 x 13.8	24

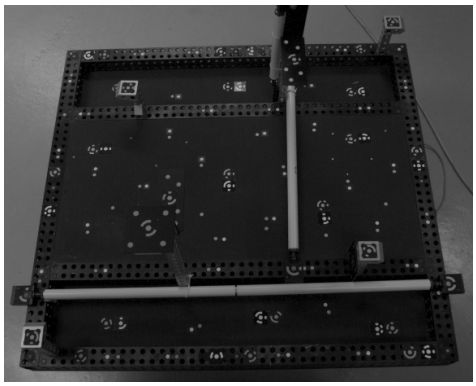

Test 1: IAPG test field

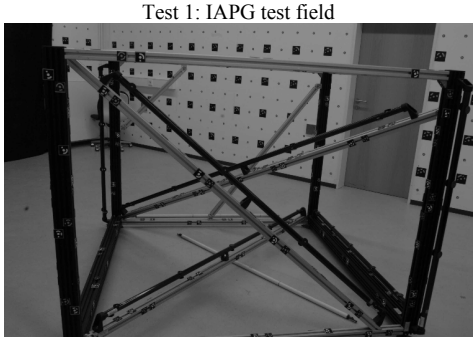

Test 2: AICON test field

Fig. 5: Test fields used for measurement

4.2 Evaluation

In the first instance, the acquired colour images are converted into separate colour channels. This step is necessary for those photogrammetric software programs that do not enable point measurements in selected colour channels. Target points are then measured in each colour channel, in the original RGB image and in the converted intensity image. Image measurements and consecutive bundle adjustment are computed with AICON 3D Studio.

In the next step a combined bundle adjustment with Ax.Ori (AXIOS 3D) is calculated using the image points of all colour channels as observations. For this process the parameters of exterior orientations of the R, G and B images are fixed for each camera station, i.e. there is only one set of exterior orientation parameters to be estimated for each physical camera position. In addition, three (virtual) cameras are introduced into the bundle adjustment in order to model individual camera parameters for each colour channel. The camera parameters c, x'_0, y'_0 and A_1, A_2, A_3 are introduced as unknowns while the parameters for decentring distortion (B_1, B_2), affinity and shear (C_1, C_2) are fixed. The object coordinate system (datum definition) is defined by free-net adjustment and optional scale information.

4.3 Results

4.3.1 Test 1

Firstly, the separate image point measurements in the three colour channels are displayed as vector diagrams. As an example, Fig. 6 displays two data sets where the differences of image coordinates between the green channel versus red and blue channel are plotted.

The vector diagram of the Canon EOS D1 shows almost no systematic effect as it is visible for the Fuji S2 Pro with a 20mm lens. This behaviour is confirmed by the computed principal distance that shows a maximum deviation of about 4µm for the Canon while it is about 27µm for the Fuji camera (see Table 2). It is assumed that the Canon lens is very well corrected for chromatic aberration.

The results of combined bundle adjustment correspond to the theoretical relationship between principal distance and longitudinal chromatic aberration as displayed in Fig. 3. Except for the Canon, all data sets of Table 1 provide shorter principal distances in blue than in red.

The major success of the presented combined adjustment is given by an improved inner system precision by an average factor of 1.7 if compared to standard processing of single colour channels or intensity images. The results have been verified by six independent data sets with different imaging configurations. The smallest improvement was achieved with 1.6 for the Fuji S2, the largest improvement was 1.8 for the Canon. The already high accuracy level of the Nikon D2X of 1:158,000 could be enhanced to a level of 1:280,000.

Canon EOS D1 with 35mm lens

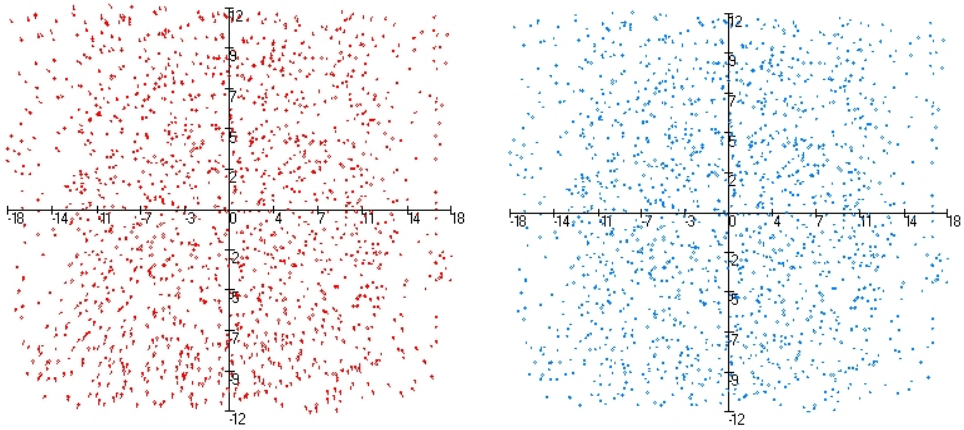

Fuji S2 Pro with 20mm lens

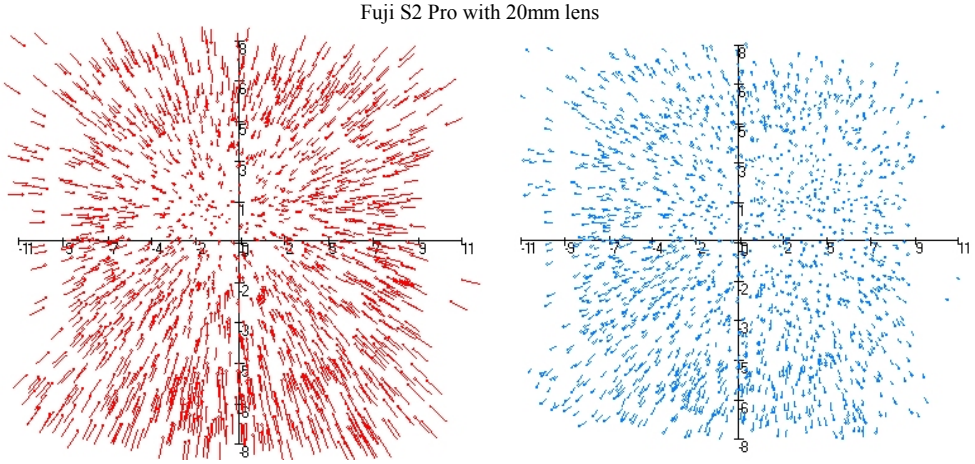

Fig. 6: Vector plots of image measurements of red (left) and blue (right) versus green

Table 2: Calibrated camera parameters after combined adjustment (Test 1)

Principal distance	c_R	c_G	c_B	s_c
Canon EOS D1 with f = 35mm	-33.3337	-33.3299	-33.3309	0.12µm
Fuji S2 Pro with f = 20mm	-20.5739	-20.5557	-20.5468	0.62µm
Principal point x'_0	x'_{0R}	x'_{0G}	x'_{0B}	$s_{x'}$
Canon EOS D1 with f = 35mm	-0.0345	-0.0342	-0.0341	0.02µm
Fuji S2 Pro with f = 20mm	0.2812	0.2818	0.2812	0.36µm
Principal point y'_0	y'_{0R}	y'_{0G}	y'_{0B}	$s_{y'}$
Canon EOS D1 with f = 35mm	-0.0494	-0.0493	-0.0490	0.02µm
Fuji S2 Pro with f = 20mm	-0.2080	-0.2095	-0.2105	0.38µm

Table 3: System accuracy after bundle adjustment (Test 1)

	[mm]	**RMS_X**	**RMS_Y**	**RMS_Z**	**RMS_{XYZ}**	**Relative precision**
Fuji S2 Pro 20mm	intensity	0.0117	0.0118	0.0179	0.0244	1:62,000
	combined	0.0071	0.0072	0.0110	0.0149	1:100,000
Fuji S2 Pro 14mm	intensity	0.0186	0.0185	0.0324	0.0417	1:36,000
	combined	0.0099	0.0097	0.0191	0.0237	1:64,000
Canon D1 35mm	intensity	0.0136	0.0136	0.0183	0.0265	1:57,000
	combined	0.0069	0.0072	0.0104	0.0144	1:105,000
Nikon D2X 24mm	intensity	0.0046	0.0049	0.0067	0.0095	1:158,000
	combined	0.0025	0.0024	0.0040	0.0053	1:285,000
Sigma SD10 24mm	intensity	0.0155	0.0153	0.0193	0.0291	1:50,000
	combined	0.0092	0.0096	0.0123	0.0181	1:83,000

4.3.2 Test 2

Test 2 was carried out mainly for testing the results with respect to the achievable length measurement error LME. The LME is the ISO-conform criteria for the absolute accuracy (not inner precision) of a coordinate measuring device. A set of calibrated reference scale bars is used to compare measured distances (calculated from measured 3D coordinates) against calibrated lengths. The LME is the only accepted way for system verification and traceability in industrial practice.

For this purpose a 3D test field provided by AICON 3D Systems has been measured by approximately 90 images. The test field consists of 160 object targets and 55 calibrated scale bars. The scale bars contain a number of sub-distances in order to increase the number of compared distances.

In general, the results of Test 1 have been confirmed. For different camera/lens combinations, the internal precision can be increased by a factor of about 1.7 in all cases. The best result was achieved with the Nikon D2X camera with 24mm lens where a relative precision of about 1:95,000 was obtained (see Table 4). In this case, the RMS point error RMS_{XYZ}, given by

$$RMS_{XYZ} = \sqrt{RMS_X^2 + RMS_Y^2 + RMS_Z^2}$$

yields to 0.022mm. With regard to the exterior accuracy the length deviations range between -0.08mm and +0.05mm (compare Fig. 7) according to an RMS_{LME} value (Table 4) with

$$RMS_{LME} = \sqrt{\frac{\sum l^2}{n}}$$

Since the LME considers all length measurements (100%), the theoretical threshold t_{LME} of all LME (calculated from 3D distances) is simplified given by

$$t_{LME} = 3 \cdot \sqrt{2} \cdot RMS_{XYZ} = \sqrt{18} \cdot RMS_{XYZ}$$

where the factor 3 is given by a 99% significance level. With a point error $RMS_{XYZ} = 0.022$mm, a length precision of $t_{LME} = 0.09$mm can be achieved. Thus, the empirically measured LME corresponds well to the theoretical limit. An increase in the exterior accuracy of factor 1.3 can be achieved using the combined calibration method.

Table 4: System accuracy after bundle adjustment (Test 2)

	Nikon D2X f=24mm		
	RGB comb.	grey scale	grey 3
Sigma 0 [µm]	0.35	0.30	0.30
RMS_X [mm]	0.013	0.023	0.013
RMS_Y [mm]	0.009	0.017	0.010
RMS_Z [mm]	0.015	0.025	0.014
RMS_{XYZ} [mm]	0.022	0.038	0.022
Rel. precision	95,000	55,000	98,000
LME	-0.08 - 0.05	-0.12 - 0.05	-0.12 - 0.05
RMS_{LME}[mm]	0.0351	0.0485	0.0482
t_{LME}	0.094	0.161	0.091

A further comparison of Test 1 and Test 2 indicates that the relative precision for the plane test field is about two times better than for the 3D test field. We assume that systematic imaging errors, e.g. radial distortion, can not be compensated by modified point coordinates for spatial point distributions and all-around imaging configurations, as it may be possible for plane point fields.

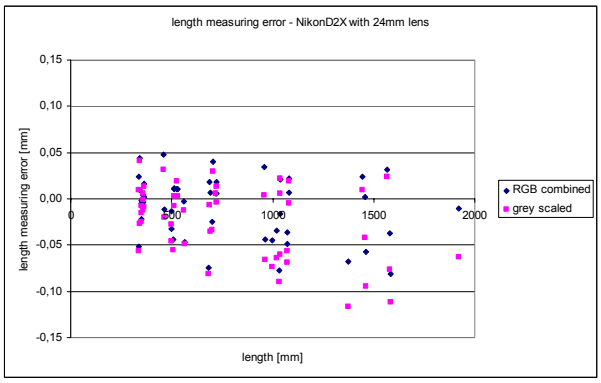

Fig. 7: Diagram of length measurement error for Nikon D2X with 24mm lens

4.3.3 Precision and design factor

According to Fraser, 1996, the relationship between object precision s_{XYZ}, image precision $s_{x'y'}$, image scale m, design factor q_D and number of images per camera station k is given by

$$s_{XYZ} = q \cdot m \cdot s_{x'y'} = \frac{q_D}{\sqrt{k}} m \cdot s_{x'y'}$$

For k=1 it is q=q_D. Separately introduced RGB channels yield k=3, i.e. with $\sqrt{3} = 1.73$ the empirical accuracy improvement of about 1.8 is confirmed. The computed examples result to a mean design factor of 0.7.

The same improvement can be achieved if the number of observations is simply increased by introducing each image point measurement three times into the bundle adjustment. However, since no additional real measurement is introduced, this is only a numerical effect where the RMS values of the adjustment get smaller by increasing the number of observations. σ_0 is not affected by the number of observations ("grey 3" in Table 4).

The correction of colour images as discussed in section 3.2 using the program PhotoShop CS2 was applied to the Nikon D2X and Sigma SD10 images. After conversion into intensity images and standard photogrammetric data processing, no improvement could be observed compared to corresponding original intensity images. Since the additional effort shows no positive effect, this approach can be rejected.

5. SUMMARY AND FUTURE PROSPECTS

This investigation was based on the assumption that the typical relative accuracy of professional colour cameras of about 1:100,000 does not represent the existing potential of high-resolution cameras (Peipe, 2005). Since instabilities of cameras during image acquisition can already be modelled by image-variant camera calibration (Tecklenburg et al., 2001) it was obvious to concentrate on the colour characteristics of cameras and lenses. Wave length dependent lens errors, different colour sensor principles and internal image processing form a complex process that is responsible for the quality of the final image.

Chromatic aberration of the lens provides significantly different images for the single RGB channels. However, this effect

should not be interpreted as a negative influence but, it shows that all three channels provide more information than a single channel. As a consequence, if separate image measurements are introduced and combined with additional constraints in object space, a significant accuracy enhancement of about factor 1.3 can be achieved. Simply spoken, three images and three cameras are used for each camera station that lead to a theoretical and practical improvement of the inner system precision of factor 1.7 (Fraser, 1996, Fraser et al., 2005). The effect on external accuracy is less significant as it has been expected. The standardized length measurement error is improved slightly without showing a strong relationship the estimated RMS values. Additional investigations are scheduled for the next months.

The presented approach is user-friendly and easy to implement since no additional software modules like a resampling correction for aberration have to be used. The processing times rise according to the time that is required for the measurement of two additional channels. In practice this will be not more than a few seconds for a complete set of images.

6. REFERENCES

Cronk, S., Fraser, C.S., Hanley, H., 2006: Automatic calibration of colour digital cameras. *The Photogrammetric Record*, to appear in 2006.

Fraser, C.S., 1996: Network design. In Atkinson (ed.): *Close Range Photogrammetry and Machine Vision*, Whittles Publishing, pp. 256 – 281.

Fraser, C.S., Woods, A., Brizzi, D., 2005: Hyper redundancy for accuracy enhancement in automated close-range photogrammetry. *The Photogrammetric Record*, Volume 20 , September 2005.

Fryer, J.G., Brown, D.C., 1986: Lens Distortion for Close-Range Photogrammetry. *Photogrammetric Engineering & Remote Sensing* (52), No. 1, pp. 51-58.

Fryer, J.G. (1996): Camera calibration. In Atkinson (ed.): *Close Range Photogrammetry and Machine Vision*, Whittles Publishing, pp. 156 – 179.

Hastedt, H., Luhmann, T., Tecklenburg, W., 2006: Zur Nutzung von RGB-Kanälen für die hochgenaue 3D-Punktbestimmung. In Luhmann (ed.): *Photogrammetrie, Lasercanning, Optische 3D-Messtechnik – Beiträge der Oldenburger 3D-Tage 2006*, Wichmann Verlag, Heidelberg.

Kaufmann, V., Ladstädter, R., 2005: Elimination of color fringes in digital photographs caused by lateral chromatic aberration. XXth International CIPA Symposium 2005.

Luhmann, T., Wendt, K. (2000): Recommendations for an Acceptance and Verification Test of Optical 3-D Measurement Systems. *International Archives for Photogrammetry and Remote Sensing*, Vol. 33/5, Amsterdam, pp. 493-499.

Luhmann, T., Robson, S., Kyle, S., Harley, I., 2006: *Close-range photogrammetry*. Whittles Publishing, Caithness, UK, to appear in 2006.

Lyon, R., Hubel, P., 2002: Eyeing the Camera: Into the Next Century. IS&T/TSID 10th Color Imaging Conference Proceedings, Scottsdale, Az., USA, pp. 349-355.

Peipe, J., 1995: Photogrammetric investigation of a 3000 x 2000 pixel high-resolution still-video camera. ISPRS Intercommission Workshop „From Pixels to Sequences“, Zürich.

Peipe, J., 2005: Entwicklungstendenzen in der digitalen Fotografie. In Luhmann (ed.): *Photogrammetrie – Laserscanning – Optische 3D-Messtechnik*. Wichmann Verlag, Heidelberg, pp. 150-155.

Pedrotti, F., Pedrotti, L., Bausch, W., Schmidt, H., 2002: *Optik für Ingenieure - Grundlagen*. Springer, Berlin, 846p.

Schröder, G., 1990: *Technische Optik*. Kamprath Reihe, Vogel Verlag, Würzburg.

Schwalbe, E., Maas, H.-G., 2006: Ein Ansatz zur Elimination der chromatischen Abberation bei der Modellierung und Kalibrierung von FishEye-Aufnahmesystemen. In Luhmann (ed.): *Photogrammetrie – Laserscanning – Optische 3D-Messtechnik*. Wichmann Verlag, Heidelberg.

Shortis, M.R., Beyer, H.A., 1996: Sensor technology for digital photogrammetry and machine vision. In Atkinson (ed.): *Close Range Photogrammetry and Machine Vision,* Whittles Publishing, pp. 106 155.

Tecklenburg, W., Luhmann, T., Hastedt, H. (2001): Camera Modelling with Image-variant Parameters and Finite Elements. *Optical 3-D Measurement Techniques V*, Wichmann Verlag, Heidelberg.